Ecological Modelling 291 (2014) 28–41

Contents lists available at ScienceDirect

Ecological Modelling

journal homepage: www.elsevier.com/locate/ecolmodel

The mangrove forest dynamics model mesoFON

U. Grueters[a,*], T. Seltmann[a], H. Schmidt[a], H. Horn[b], A. Pranchai[a,c], A.G. Vovides[a,d], R. Peters[a], J. Vogt[a], F. Dahdouh-Guebas[e,f], U. Berger[a]

[a] Department of Forest Biometry and Systems Analysis, Institute of Forest Growth and Forest Computer Sciences, Technische Universitaet Dresden, Postfach 1117, 01735 Tharandt, Germany
[b] Department of Forest Growth and Forest Mensuration, Institute of Forest Growth and Forest Computer Sciences, Technische Universitaet Dresden, Postfach 1117, 01735 Tharandt, Germany
[c] Department of Silviculture, Faculty of Forestry, Kasetsart University, 50, Chatuchak, Bangkok 10900, Thailand
[d] Red de Ecología Funcional, Instituto de Ecología, A.C., Carretera Antigua a Coatepec 352, Xalapa 91070, Veracruz, Mexico
[e] Laboratory of Systems Ecology and Resource Management, Department of Organism Biology, Université Libre de Bruxelles – ULB, Av. F.D. Roosevelt 50, CPI 264/1, B-1050 Brussels, Belgium
[f] Laboratory of Plant Biology and Nature Management, Department of Biology, Vrije Universiteit Brussel – VUB, Pleinlaan 2, B-1050 Brussels, Belgium

ARTICLE INFO

Article history:
Received 26 November 2013
Received in revised form 11 July 2014
Accepted 14 July 2014

Keywords:
Individual-based model
Field-of-neighborhood
Plant functional type
Mangroves
Rhizophora mangle
Hurricane impacts

ABSTRACT

This study presents mesoFON, an individual-based mangrove forest dynamics model that advances beyond current models by describing crown plasticity of mangrove trees. The crown plasticity routines take advantage of the fields-of-neighborhood (FON) approach and account for the trunk bending and the differential side branch growth mechanism. Competition for above-/below-ground resources is dealt with separately in this model. Offspring production depends on tree growth and rises with tree ontogeny.

An extensive sensitivity analysis revealed that mesoFON resembles the behavior of known mangrove forest dynamics and is ready for application.

In this study we exposed two plant functional types (PFTs) of the red mangrove (*Rhizophora mangle* L.) either in monoculture or as a community to two disturbance regimes, namely (1) without disturbances and (2) with hurricane impacts returning every 5 years. While one functional type possesses plastic crowns, the other PFT has rigid crowns. For the first time, long-term interaction of lateral crown displacement and disturbance was examined using a comprehensive comparative analysis including point patterns and canopy coverage.

In the monoculture experiments disturbance strongly promoted the beneficial effects of crown plasticity. Without disturbance crown movements merely increased stand-based stem volume by 6.7% despite considerable displacement distances. We attribute this to the overall high competitive strength that constrained the effects of plasticity in the dense stands. Yet, in disturbed stands the plastic behavior raised stem volume and tree density by 12.5% and 7.5%, respectively, as a result of substantially reduced local competition (by 20.1%). In this treatment crown shifts are particularly advantageous because of their contribution to gap closure. Generally, the Clark Evans aggregation index of crown centers tended to be higher than that of stem bases indicating a more regular distribution of crown centers. The same was true for the canopy coverage of crowns located at their centers implying better space usage by shifted crowns.

Pair-correlation functions revealed a plasticity-induced trend toward more regular distribution at low tree-to-tree distances and less aggregation at intermediate distances. The trend was stronger in disturbed communities. The plastic PFT was finally able to out-compete the rigid PFT in all community experiments. Hurricane impacts, however, accelerated the time to the extinction of the rigid PFT by a factor of 2.4.

© 2014 Elsevier B.V. All rights reserved.

1. Introduction

One of the primary objectives of individual-based modeling is to enhance our understanding of how the population or community-scale long-term system behavior of a natural forest emerges from the adaptive behavior of individual trees over their life-cycle

* Corresponding author. Tel.: +49 35203 38 31625; fax: +49 35203 38 31632.
E-mail address: Uwe.Grueters@forst.tu-dresden.de (U. Grueters).

http://dx.doi.org/10.1016/j.ecolmodel.2014.07.014
0304-3800/© 2014 Elsevier B.V. All rights reserved.

(modified after Grimm and Railsback, 2005). Mature trees, depending on their fitness, produce a larger or smaller number of seeds that disperse away from the parental tree and then establish themselves somewhere else and grow to maturity again, thereby completing their life cycle.

Plants, and especially trees, are known to exhibit adaptive behavior (Bradshaw, 2006; Valladares et al., 2007). They cannot take to their heels as animals do (Borges, 2008), but morphological plasticity enables trees to move as well. The height growth strategy that characterizes the "tree" life form is seen as an evolutionary response to the competition for light (Grams and Andersen, 2007). The most noticeable response in dense forest stands is massive stem elongation, however, the most general adaptive response of trees limited by the light resource is lateral growth of crowns toward spaces with higher light availability (Muth and Bazzaz, 2002; Trewavas, 2005; Grams and Andersen, 2007). In consequence of this response, crown centroids often do not match the location of their stem bases. They are displaced in a direction opposite to spaces of most severe competitive pressure and to a distance that depends on the prevailing neighborhood asymmetry. (Brisson, 2001; Muth and Bazzaz, 2002; Longuetaud et al., 2008, 2013; Schröter et al., 2012). Crown centers of mass were found to be more regularly distributed than stem bases and crown areas located at their centers overlapped less as if they were located at their stem bases (Longuetaud et al., 2008; Schröter et al., 2012). These results from field studies only suggest beneficial effects on the fitness of individual trees, while modeling and simulation of crown plasticity has demonstrated positive effects on stand biomass accumulation (Vincent and Harja, 2007), stand productivity and biomass (Sorrensen-Cothern et al., 1993). Umeki reported species-specific differences in the crown plasticity response over a tree's lifetime (Umeki, 1997) and species-dependent antagonistic effects of size-asymmetric competition and crown plasticity (Umeki, 1995a, 1997). These results could be obtained only through simulation due to the large spatial and temporal scales of the processes involved.

A number of models for terrestrial forest ecosystems, incorporating crown plasticity, have been developed over the past two decades. These models vary in their structural resolution and simplification of the crown as a moving zone of influence (Umeki, 1995a, 1995b, 1997), a stack of independently growing disks (BALANCE model, Grote and Pretzsch, 2002) with disk sectors representing individual branches (WHORL, Sorrensen-Cothern et al., 1993), a 3D-tesselation cell (Strigul et al., 2008; Strigul, 2012) or even a complex three-dimensional geometrical shape (as in the functional–structural model of Vincent and Harja (2007)). Plastic versions of the most widespread individual-based model (IBM) of terrestrial forest dynamics, such as SORTIE, have also been built (Plastic SORTIE, Strigul et al., 2008, LES model, Strigul, 2012). This incorporation of plasticity overcame the long acknowledged shortcoming of the assumption in SORTIE of rigid cylindrical crowns, explicitly that trees were distributed unnaturally clumped and that the model predicted far too little canopy coverage, even though the model resembled species composition and biomass of old-growth forests considerably well (Pacala et al., 1996; Strigul et al., 2008; Strigul, 2012).

In stark contrast to the previous models rigidity of crowns is still the underlying assumption in individual-based models of mangrove forest dynamics, such as FORMAN (Chen and Twilley, 1998) and KiWi (Berger and Hildenbrandt, 2000), despite the well-known plasticity of mangroves, both above- and below-ground (Tomlinson, 1994). This lack of morphological plasticity has been identified as a major limitation of current mangrove IBMs (Berger et al., 2008).

Unfortunately sound empirical data about crown plasticity of mangrove trees is still missing. Therefore, we undertook a simple approach to simulating mangrove crown plasticity. We introduce the mesoFON model that exclusively takes advantage of the fields-of-neighborhood (FON) approach that has previously been employed to address competition among trees in the KiWi model (Berger and Hildenbrandt, 2000). The extent of lateral crown movement will be regulated by a set of species-specific scaling coefficients that can be determined with ease from field measurements of crown projections in the future. We no longer treat production of offspring as constant or density-dependent, but consider it an individual-based process thereby narrowing the gap in the tree's life-cycle inherent to other models (Chen and Twilley, 1998; Berger and Hildenbrandt, 2000), enabling our model to simulate the effects of crown plasticity on a tree's fitness.

First, we will subject mesoFON to extensive evaluation and sensitivity analysis. We grow two plant functional types (PFTs) of the red mangrove (*Rhizophora mangle* L.) either in monoculture or as a community in the first application. The PFT_plastic functional type possesses plastic crowns, while PFT_rigid has rigid crowns. Since hurricanes have likely shaped the structure of most mangrove forests (Smith et al., 2009) the stands are exposed to two disturbance regimes, With_Disturbance (hurricane impacts returning every 5 years) and Without_Disturbance (no hurricanes). We examine, for the first time, the long-term effects of lateral crown displacement on forest stand dynamics through a comprehensive comparative analysis that includes point patterns and canopy coverage.

Our comparison of the behavior of the PFT monocultures addresses two questions. First, whether crown plasticity enhances the carrying capacity or reduces the competitive strength of the system in the long-term; and second, whether disturbance alters this dichotomy. The community experiments will clarify whether PFT_plastic dominates over PFT_rigid and whether hurricane impacts alter that pattern.

2. Materials and methods

The model is outlined following the ODD (overview, design concepts, details) protocol for describing individual- and agent-based models (Grimm et al., 2006, 2010).

2.1. mesoFON model ODD protocol

2.1.1. Purpose

mesoFON is a simulation model in which a mangrove forest stand emerges from the recruitment, establishment, growth, and death of individual trees. Each tree is affected by its local environmental conditions, the impact exerted by competition of neighboring trees, and by small-scale disturbance events. The crowns of PFT_plastic mangrove trees exhibit morphological plasticity in this IBM, for the first time. Lateral crown displacement is fully integrated with above-/below-ground competition through a duplicated FON approach.

We provide only a parameterization for the red mangrove in this paper; however, mesoFON can house up to 10 species via the GUI and the number of species can be further enlarged with little coding effort (compare Appendix B in Supplementary Material). Parametrizing other mangrove species of the Atlantic-East Pacific or the Indo-West Pacific Region (such as *Avicennia germinans*, *Kandelia obovata* Sheue, Liu & Young, *Laguncularia racemosa* (L.) Gaertn.f., *Rhizophora apiculata* Bl.) is straightforward. Our instructions and the descriptions from Berger and Hildenbrandt (2000), Fontalvo-Herazo et al. (2011), Kautz et al. (2011) and Khan et al. (2013) can assist users in accomplishing these parameterizations. The original KiWi model has proven to be an excellent tool for the study of theoretical and applied ecological questions regarding

mangrove forest dynamics. mesoFON is built upon KiWi; therefore, it should also prove useful in further research.

2.1.2. Entities, state variables and scales

In the simulations we follow the dynamics of red mangrove forest stands on 2 ha over a period of 8000 years at annual time steps. The state of a tree is defined in the model by the *x*,*y*-position of its stem base, the shifted *x*,*y*-position of its crown centroid (differs from the first variable only for trees of PFT_plastic), the diameter at breast height (dbh at 1.37 m height), age and the Δdbh of the five years prior to the current simulation year. Additional derived variables, such as the crown displacement distance, tree height (h), basal area and stem volume, are calculated from the state variables. These variables are then scaled up to attain stand state variables recommended for the "Standard Analysis of Long-Term Experimental Plots" (Pretzsch, 2009).

2.1.3. Process overview and scheduling

Four fundamental processes are accounted for and scheduled in the following order: (1) tree recruitment, i.e. propagule production and dispersal (2) tree establishment and growth as modified by competition and environment, (3) crown displacement away from the most severe competitive pressure and (4) both, natural and disturbance-related mortality.

(1) Offspring production depends on the size of an individual tree and is down-regulated in situations of low tree growth. The offspring establishes in the stage of standardized saplings at an initial dbh of 2.5 cm and an initial height of 327.7 cm, respectively. Offspring are placed at uniformly distributed random locations on the plot, i.e. we assume global dispersal.
(2) The analysis of tree rings is generally less straightforward in the tropical zone than in the temperate zone due to the lack of a demarcated unfavorable winter season in the tropics. Because of the involved difficulties "the use of growth rings for mangrove age or growth rate determinations should be evaluated on a case by case basis" (Robert et al., 2011). Therefore we adhere to the Shugart growth function that is not directly dependent on tree age (Shugart, 1984). After taking into account competition, the limitation of available light, pore water salinity, and nutrient levels constrain this optimal growth (Berger and Hildenbrandt, 2000, according to Chen and Twilley, 1998). Our objective to incorporate crown plasticity into the model required that we distinguish between competition for above- and below-ground resources. Therefore, in mesoFON each tree is surrounded by two circular fields of neighborhood. The intensity of the above-ground FON declines sharply (and exponentially) with distance from the trunk to the FON-radius, to simulate size-asymmetrical competition for light. In contrast, the second FON, which mimics the rather size-symmetrical below-ground competition, has almost constant intensity.
(3) A cause and effect relationship is established by coupling movements of above-ground FONs and crowns. Each above-ground FON stores the competitive influence of all overlapping neighbor fields along with their coordinates. Vectors of neighborhood asymmetry (Muth and Bazzaz, 2002) can be calculated from this information to give crown movement direction and extent. Above-ground FON and crown must operate as a functional unit over the entire lifespan of a tree. For that purpose, their dimensions must remain proportional during ontogeny.
(4) Tree death occurs in the model for one of two reasons, either the mean Δdbh of the preceding five years falls below the species-specific threshold or a local disturbance event, say a hurricane, hits the tree.

After all the individual trees have completed their actions the stand state variables are synchronously updated.

2.1.4. Design principles

2.1.4.1. Emergence. The macro-scale behavior of the stand that emerges from the micro-scale processes at the level of organisms is represented by the dynamics of the following stand state variables: tree density, stand basal area (SBA), stem volume of the stand (V, assuming a form factor of 0.43 for red mangrove), and quadratic mean dbh of the whole stand (d_q) and the 100 thickest trees in the stand (dbh100).

2.1.4.2. Sensing and interaction. An established red mangrove tree senses the influence and identity/position of competitors inside its above- and below-ground FON surrounding and thereby interacts with its neighbors. Below-ground, it probes the environment at the position of its trunk origin and acts accordingly. In contrast, above-ground probing of the environment takes place at the center of the crown and is affected by its displacement. Above-ground, all the vectors of the normed competitors' intensities are added up to find the direction of maximum competitive influence. The center of the crown together with that of the above-ground FON is moved in the opposite direction.

2.1.4.3. Stochasticity. Positions of the produced saplings are chosen randomly. Moreover, disturbance events occurring at pre-defined frequency impact a fraction of the individual trees at random.

2.1.4.4. Observation. Six displays (see Fig. 1) and a number of charts are provided in the mesoFON model to keep visualization in balance with model complexity. A 3D-display (top-center, of Fig. 1) allows for an intuitive surveillance of the virtual forest stand. A tree is realistically dimensioned in this display. It is represented by a spherical crown, a disk-shaped below-ground FON and a cylindrically-shaped trunk, respectively. Additional 2D-displays are available for the dimensions of above-/below-ground FONs (top-left, top-right). Distinguishing between the functional types is possible in those three displays, because trees and tree components (crowns or FONs) are shown with a specific color for each type. Two other fine-grained 2D-displays show the intensity of competition above- or below-ground at grid points 1 m apart from each other (bottom-left, bottom-right). The displacement display (bottom-center) shows crown projections centered at stem bases in brown and shifted crown projections in green. Labels indicate displacement distances in meters. All these displays allow the user to inspect the state of selected individual trees. The mesoFON-GUI also includes line diagrams that depict time-courses of "species-specific" and total stand state variables. Additionally, the model provides file outputs containing stand state variables every year and state variables for all the trees present every 500 years.

2.1.5. Initialization and input

Initially, the plot area is populated with randomly placed saplings, the number of which the user can freely select. In most model runs 750 randomly located saplings were placed into the virtual plot. Gray-scale image maps of light availability, pore water salinity and nutrient level represent abiotic conditions in a spatially-explicit way. In this study, however, all simulation experiments are run in a homogeneous optimum environment.

2.1.6. Submodels

2.1.6.1. Tree recruitment. Recruitment involves the annual production of offspring by parental trees, the number of which (N) is given by the following formula:

$$N = f_{\mathrm{red}} \cdot D \cdot A \quad (1)$$

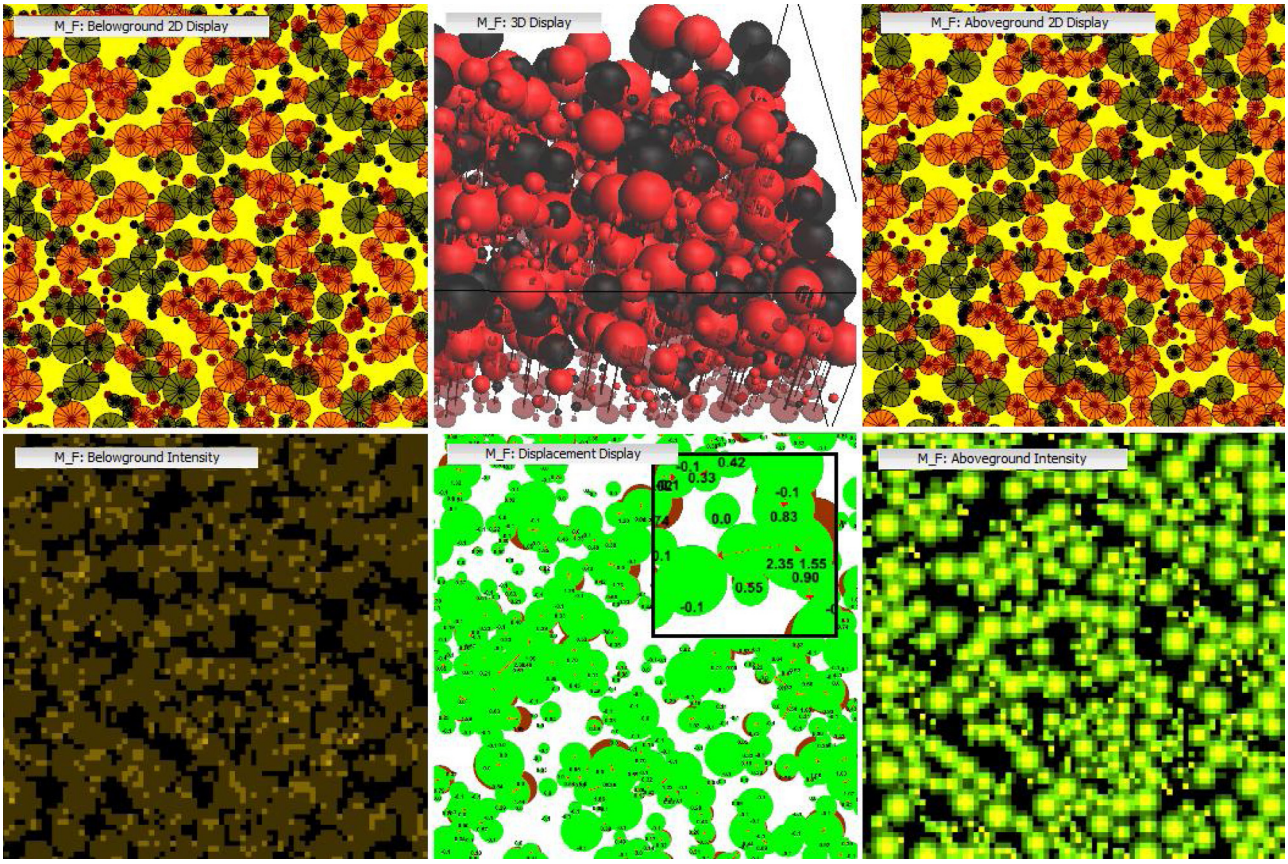

Fig. 1. The mesoFON displays. 3D-display of the virtual mangrove forest stand (top-center), 2D-displays of below-ground FONs (top-left), below-ground FON-intensity (bottom-left), above-ground FONs (top-right), above-ground FON-intensity (bottom-right), displacement display (bottom, in the middle) with enlarged section, brown circles represent crown projections located at stems, green circles are crown projections located at their centers, arrows depict displacement vectors, labels denote displacement distances in meters. (For interpretation of reference to color in this figure legend, the reader is referred to the web version of this article.)

where f_{red} is a reduction factor and D is the offspring density per crown surface area A in [m^2].

R. mangle propagules due to their size are clearly identifiable from distance, therefore, propagule density per crown surface area was considered a suitable parameter to employ now and to measure in the future. However, since the Shugart growth function and the FON algorithm require us to insert new juvenile trees in a sapling stage, the "fictive" density employed here represents number of saplings rather than number of propagules per crown surface area. Therefore, the procedure ignores the "self-thinning" of seedlings. With D set to 0.006 per m^2 we attained stem volumes that were similar to those reached by stands with the commonly applied 30 saplings per ha and year (Chen and Twilley, 1998). The deterministic approach used here accumulates sapling numbers per tree as decimal numbers, but trees only produce integer numbers of saplings, while the fractional remainder is kept for later. This procedure ensures that the annual offspring production of an individual tree increases during its ontogeny. However, we reduced offspring production in years of low growth rate using the same factor f_{red} as in Eqs. (2), (4), and (8) to avoid the biologically unrealistic behavior that a tree, under unfavorable conditions, produces more offspring over its lifetime, simply because it lives longer than it would have under favorable conditions (see Appendix C in Supplementary Material).

2.1.6.2. Tree growth. mesoFON adopts an optimum growth formulation for an individual tree that is reduced by the local environment and the competition from neighboring trees. The concept is best illustrated by the basic equation for annual stem volume growth that both Botkin et al. (1972) and Shugart (1984) use at the beginning of their descriptions:

$$\frac{\Delta(d^2h)}{\Delta t} = \left[R \cdot LA \cdot \left(1 - \frac{d \cdot h}{d_{max} \cdot h_{max}}\right)\right] \cdot f_{red} \quad (2)$$

where d is the diameter at breast height [cm] of a focal tree, d_{max} is the maximum attainable dbh in cm, h is the tree height [cm], h_{max} is the maximum achievable height [cm], LA is the leaf area [cm^2] of the tree and R is a constant that characterizes the function of the leaf area in terms of volume growth, while f_{red} represents the reduction of stem volume growth due to environment and competition.

In the first term ($R \times LA$) the equation, in principle, assumes a linear relationship between stem volume growth and leaf area, whereas the second term ($1 - d{\cdot}h/(d_{max}{\cdot}h_{max})$) has a constraining influence that reflects rising maintenance requirements of the trunk for a larger tree. Growth terminates entirely, when a tree reaches its d_{max} and h_{max}. The Shugart growth function is particularly suitable for mangroves, because tree growth does not depend on tree age (that is difficult to assess, Robert et al., 2011), but is based merely on the current dbh. Furthermore, the estimation of its few parameters is straightforward even for the common situation of data scarcity in mangroves.

We assume that the derived variable tree height is given by the following height vs. dbh function (Berger and Hildenbrandt, 2000; Shugart, 1984; Botkin et al., 1972):

$$h = 137 + b_2 d - b_3 d^2 \quad (3)$$

with b_2 and b_3 being two growth function parameters.

Inserting Eq. (3), assuming further that specific leaf area stays constant during ontogeny and leaf weight $LW = C \times d^2$ yields the ultimate annual dbh increment function:

$$\frac{\Delta d}{\Delta t} = \left[G \cdot d \cdot \frac{\left(1 - \frac{d \cdot h}{d_{max} \cdot h_{max}}\right)}{234 + 3b_2 d - 4b_3 d^2} \right] \cdot f_{red}, \quad \text{with } G = R \cdot C \tag{4}$$

where G is another growth parameter that denotes the initial growth rate of a sapling and h is the tree height as calculated by Eq. (3).

Eq. (4) can be classified as a saturating function that asymptotically approaches d_{max}.

2.1.6.3. Competition among trees. This section provides details of the "field of neighborhood" (FON) approach. The equations are derived from Berger and Hildenbrandt (2000). Extensions with respect to the separation of competition into above- and below-ground parts are also given.

At radius r [m] the intensity of competition exerted by a tree is given by

$$\text{FON}(r) = \left\{ \begin{array}{l} \text{for } 0 < r < rbh \rightarrow I_{max} \\ \text{for } rbh < r \leq R_{FON} \rightarrow \frac{I_{max}}{e^{c \cdot rbh}} \cdot e^{c \cdot r}, \quad c = \ln \frac{I_{min}}{R_{FON} - rbh} \\ \text{for } r > R_{FON} \rightarrow 0 \end{array} \right\} \tag{5}$$

where rbh is the radius at breast height [m], R_{FON} is the radius [m] of the FON, I_{max} is the maximum intensity of competition (inside the trunk), I_{min} is the minimum intensity of competition at R_{FON}, defined as a fraction of I_{max}.

The structure of Eq. (5) ensures that the FON intensity declines exponentially from I_{max} at the trunk to I_{min} at the FON margin.

The increase in the FON radius [m] with increasing tree size is governed by the following allometric relationship:

$$R_{FON} = a \cdot (rbh)^b, \quad a = 7.113 \quad \text{and} \quad b = 0.654 \tag{6}$$

where allometric coefficient a and allometric exponent b are set to values identical with those of the crown allometry (Berger and Hildenbrandt, 2000). Please note, that the exponent b and the allometry of Eq. (6) is only valid when rbh stays below 1 m.

The local intensity of competition at an x,y-location in the plot area is given by Eq. (7). In principle it is obtained by adding the intensities of all n FONs that have non-zero intensity at x,y and overlap with the coordinate.

$$F(x, y) = \sum_n \text{FON}_n(x, y) \tag{7}$$

The competitive influence F_A^k of n neighboring trees ($n \neq k$) on a focal tree k is then calculated by summing the area-based integrals of all n FON overlaps and dividing each by the integral of the focal FON to normalize it:

$$F_A^k = \sum_{n \neq k} F_{A_k}^n = \sum_{n \neq k} \frac{\int_{A_k} \text{FON}_n(x, y) da}{\int_{A_k} \text{FON}_k(x, y) da} \tag{8}$$

where A_k is the FON area of the focal tree and da is the area variable over which we are integrating.

F_A^k is scaled to a range of [0,1] in case the value calculated by Eq. (8) falls outside this range. The generalized normalization step described above is applicable to any I_{max} and I_{min} parameter values. The separation into above- and below-ground competition claimed for such a generalization as outlined below.

2.1.6.4. Separation into above-/below-ground competition. A prerequisite for the implementation of crown plasticity was a separation of competition into above- and below-ground competition. In accordance with other individual-based forest growth models (SORTIE, Deutschman et al., 1997) we aimed to give above-ground competition a far greater weighting than that operating below-ground. Assuming further that competition for sunlight is highly asymmetrical (Grams and Andersen, 2007) we assigned the above-ground I_{max} parameter to 0.95 and I_{min} to 0.07, i.e. the intensity of a competitive field drops sharply from 0.95 at the trunk to 0.067 (in absolute terms) at the FON radius.

In contrast, competition for below-ground resources is considered to be rather size-symmetrical (Casper and Jackson, 1997), in particular, when the nutrient under investigation was rather mobile and had a non-patchy distribution in the soil volume (Grams and Andersen, 2007). We assume here a sound mobility of all the limiting factors in the *R. mangle* rhizosphere (see Section 4 for a detailed derivation) and infer a completely symmetrical type of below-ground competition at an overall low intensity. In line with that I_{max} was assigned to 0.05 and I_{min} to 0.999 (≈0.05 in absolute terms).

2.1.6.5. Combined effects of competition and environment on growth. In principle, above- and below-ground FON intensities ($F_{A,above}^k$, $F_{A,below}^k$) are considered to impact the growth of a focal tree additively. The level of incoming sunlight (above the canopy) is assumed to be optimal and does not constrain the growth. The influence of salt ($f_{red,Salt}$) and nutrient levels ($f_{red,Nut}$) on tree development is calculated as described in Chen and Twilley (1998). The resulting reduction of tree growth due to the combination of competition and environment is then given by:

$$f_{red} = (F_{A,above}^k + F_{A,below}^k) \cdot f_{red,Salt} \cdot f_{red,Nut} \tag{9}$$

A salinity of 30 g kg^{-1} and a total phosphorus concentration of 146.8 g m^{-2} soil area to a depth of 40 cm were chosen for the model runs. The chosen values ensure a maximum possible red mangrove growth, although the $f_{red,Nut}$ multiplier remains at about 0.6 in that case.

2.1.6.6. Crown plasticity. In the current version of the model only mangrove trees belonging to the plastic functional type (PFT_plastic) are able to displace their crowns. Generally, meso-FON implies that a tree crown is of a spherical form and that its radius (R_{crown}) like that of the above-ground FON scales with the rbh of the trunk as $R_{crown} = 7.113 rbh^{0.654}$. In principle, two processes are considered to contribute to the translocation of a crown: First, a trunk might bend away from a neighbor tree; second, side branches defining the crown margin might grow differentially depending on the vicinity of neighbor trees.

To accomplish the adaptive behavior the vector opposing the maximum competitive influence $\overrightarrow{V_{comp,k}}$ on a focal tree k is found by:

$$\overrightarrow{V_{comp,k}} = \sum_n \widehat{\overrightarrow{Pos_{shift,k}(x, y)} - \overrightarrow{Pos_{shift,n}(x, y)}} \cdot F_{A_{k,above}}^n \tag{10}$$

The vector of the shifted position $\overrightarrow{Pos_{shift,n}(x, y)}$ is subtracted from the shifted position vector $\overrightarrow{Pos_{shift,k}(x, y)}$ of the focal tree for each of the n overlapping above-ground fields; the resulting vector is normalized ($\widehat{\ }$) and scaled by the competitive intensity $F_{A_{k,above}}^n$ of the nth FON. Finally, a summation of the vectors is assumed to give $V_{comp,k}$.

The vector of translation due to trunk bending $\overrightarrow{V_{bend,k}}$ is given by:

$$\overrightarrow{V_{bend,k}} = min(\vec{u}, sc_{bend} \cdot \overrightarrow{V_{comp,k}}) \cdot tan\alpha_{max} \cdot \Delta h \tag{11}$$

where $\vec{u}$ is a unit vector pointing in the same direction as $\overrightarrow{V_{comp,k}}$, Δh is the tree height growth of the simulation year, α_{max} denotes the maximum trunk inclination angle for the species under study and

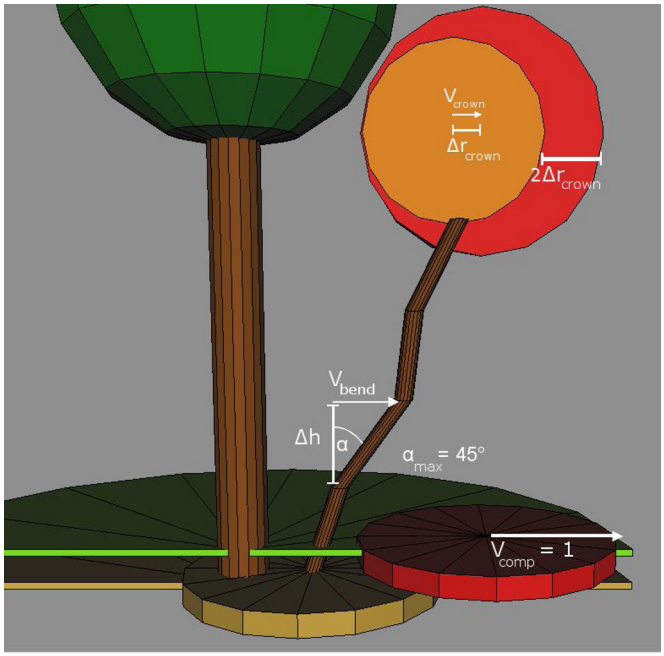

Fig. 2. Graphical illustration of the maximum crown shift routines: On the left a large normal tree with its crown, trunk and cut above-/below-ground FONs is shown. On the right is a small tree with growing crown and the capability to shift its crown. Because both of its FONs are entirely overlapped by the larger tree it experiences maximum competitive pressure. Hence, its competition vector V_{comp} has a length of 1 and points away from its neighbor. Crown shift by bending is shown on the right trunk for a previous year. In the same extreme competitive situation α equals 45° and the crown center has shifted away due to trunk bending by the vector V_{bend} wirth the same length as the height growth Δh of that year. Crown shift due to differential side-branch growth (shown on the left crown) is also extreme: The center shifts away by the vector V_{crown} having the length of crown radius growth Δr of this year.

sc_{bend} represents a species-specific scaling coefficient that enables fitting trunk bending to field data.

We assessed from visual inspection of red mangrove images that the maximum bending angle of trunks is 45° (roughly).

A similar equation obtains the vector of crown movement due to differential side branch growth:

$$\overrightarrow{V_{crown}} = \min(\vec{u}, sc_{crown} \cdot \overrightarrow{V_{comp,k}}) \cdot \Delta R_{crown} \quad (12)$$

with ΔR_{crown} representing the crown growth rate of the simulation year, and sc_{crown} again being a species-specific scaling coefficient for the kind of displacement.

The minimum function in both equations ensures that the length of $\overrightarrow{V_{comp,k}}$ ranges between 0 and 1. Therefore, given the above parameters, crown centers of red mangroves can move a maximum of Δh and ΔR_{crown} each year. Both species-specific scaling coefficients were assumed to have a value of 5 in the simulation runs. Fig. 2 illustrates the implementation concepts for the case of maximum displacement.

2.1.6.7. Tree death. Natural and disturbance-related tree death are distinguished in the mesoFON model. Trees exhibit natural death when the average annual dbh increment falls below a threshold of 0.2 cm/year. This occurs solely from "mechanistic" causes (ignoring mortality by chance), either from slowing of tree growth at the end of a tree's lifespan or from competitive exclusion.

The parameters for disturbance-related tree death were set with guidance from data of the U.S. National Weather Service (National Hurricane Center, 2013). The National Hurricane Center reports "Estimated return period in years for hurricanes (≥100 km/h) passing within 50 nautical miles of various locations on the U.S. Coast" in the range of 5–18 years. We chose a With_Disturbance treatment applying a hurricane return period of 5 years and a 10 percent tree mortality rate per event to cover the maximum range of possible interactions between disturbance regime and crown plasticity. We compare this to a Without_Disturbance treatment in the following analyses.

mesoFON has been implemented using the agent-based modeling framework RePast Simphony/Java (North et al., 2013) and will be made available as open-source software on the web (http://www.mesofon.org). Appendix A in Supplementary Material contains a screenshot of the mesoFON parameter pane with the entire parameter set that was used for this article. Appendix B in Supplementary Material provides the software requirements specification that guided our mesoFON development.

2.2. Simulation experiments and their analysis

Basically, three kinds of simulation experiments were conducted in this study: (1) sensitivity analysis; (2) monocultures, with either the plant functional type having rigid crowns or with the PFT possessing plastic crowns; and (3) communities that had both PFT_rigid and PFT_plastic functional types.

All simulation experiments were run on a personal computer with an Intel® Core™ i5-2410M processor at 2.3 GHz clock frequency and 8 GB RAM and on two virtual machines equipped with Intel® XEON® dual-core processors, 3.06 GHz, 4 GB RAM, hosted on a XenServer (Citrix Systems, Inc., Ft. Lauderdale, USA). All computers were running the Windows 7, 64bit operating system (Microsoft Corporation, Richmond, USA).

2.2.1. Sensitivity analysis

We first carried out a local sensitivity analysis (SA), in which parameters were varied one at a time (OAT-SA), to get an overview of the model's behavior. Awareness of criticism concerning OAT-SA (Saltelli, 1999), led us to choose the configuration of the SA carefully to avoid errors and varied the parameters in the presumably linear range of ±10% about a default setting.

The default setting used with KiWi parameters was repeated to ensure consistency with previous KiWi-SA (Kautz et al., 2011; Vogt, 2012). Therefore, the SA runs differed from the latter simulation experiments in the following respects: (1) parameters of the FON radius allometry: $a = 18.0$, $b = 0.83$; (2) parameters for maximum/minimum FON intensities: $I_{max,above} = 0.9$, $I_{min,above} = 0.011$, $I_{max,below} = 0.1$, $I_{min,below} = 0.9$; (3) exclusion of disturbance by hurricanes. The purpose of this first SA part was to verify that our implementation resembled KiWi behavior. Subsequently, the SA was repeated with a default setting that took into account 10% tree mortality by hurricane impacts every five years. This second SA part included the newly introduced parameter set containing disturbance frequency/intensity and propagule production variables. These model runs were repeated five times on 4 ha plots over 10,000 years or until only one plant functional type had survived. The average system behavior was collected over the simulation period starting at 2000 years. The response of all stand state variables to the parameter variation is displayed in table form using the data visualization capabilities of MS Excel 2010 (Microsoft Corporation, Richmond, WA USA). A total of 370 SA runs were performed. The overall computational time spent on these runs was about 20 days, as 500 simulation years took around 4 min to execute.

2.2.2. Monoculture experiments

Monoculture stands consisting of either PFT_rigid or PFT_plastic were exposed to both disturbance regimes. We conducted a comparative analysis of the stand-level stem volume, the tree density as well as the average competition a tree experienced from one neighbor tree. The analysis encompasses the period in which the stand had reached a steady state, i.e. the simulation years 1000–8000.

Table 1
Results of the sensitivity analysis. For an explanation see text.

Stand State Variables:	Density (ha^{-1}) mean = 250.82		V (m^3) mean = 262.53		SBA (m^2) mean = 18.90		Dq (m) mean = 0.31		DBH100 (m) mean = 0.48	
Parameter	-10%	+10%	-10%	+10%	-10%	+10%	-10%	+10%	-10%	+10%
b2										
b3										
g										
dhmax										
b										
a										
l max										
l min										
No. Seeds										
Abs(Min)/Abs(Max):	20.5888	24.9917	18.8533	22.1293	19.2730	22.9612	13.6326	4.8356	10.6385	8.9954
Range:	-25.0	25.0	-23.0	23.0	-23.0	23.0	-14.0	14.0	-11.0	11.0
	mean = 194.221		mean = 167.274		mean = 12.803		mean = 0.290		mean = 0.400	
Parameter	-10%	+10%	-10%	+10%	-10%	+10%	-10%	+10%	-10%	+10%
seedDensity										
disturbanceFreq										
disturbanceIntens										
Abs(Min)/Abs(Max):	15.758	14.436	7.591	6.658	6.994	6.079	6.008	4.879	3.481	2.959
Range:	-16.0	16.0	-8.0	8.0	-7.0	7.0	-7.0	7.0	-4.0	4.0

Respective experiments were run with two repetitions. A linear mixed effects model was fitted to each of the stand state variables by the "lme"-function of the nlme-package in the statistics software R (Pinheiro et al., 2012; R Development Core Team, 2012). The sole fixed effect was "PFT", whereas temporal pseudo-replication was accounted for by treating it as a random effect (random = ~ years|run).

Distribution patterns of displacement distances were compared for various tree size classes in selected simulation years. Both, absolute and relative distances (i.e. absolute distance divided by the crown radius), were included in these comparisons.

Moreover, spatial point pattern analyses of original and shifted tree/crown positions were carried out using the spatstat-package in R (Baddeley and Turner, 2005). The method we used in these analyses was the aggregation index R by Clark and Evans (1954).

We took screenshots of the canopy coverage shown by shifted crowns and by crowns located at their stem bases in two PFT_plastic runs, one With_Disturbance and one Without_Disturbance. The interval among the four consecutive screenshots in each run was set to greater than 50 simulation years to reduce temporal autocorrelation. The canopy coverage was determined using the image analysis software GIMP (Peck, 2008). We calculated the sum of all crown areas every 500 years in those treatments as a reference.

2.2.3. Community experiments

In these experiments a mixture of PFT_rigid and PFT_plastic saplings was planted at model initialization. Sapling numbers were set to 50/700, 150/600, 250/500, 375/375, 500/250, 600/150, 700/50 for PFT_rigigd and PFT_plastic, respectively, to cover a range of initial conditions. Each run was repeated twice. The time-course of the most comprehensive stand state variable, i.e. the stand-based stem volume, was portrayed by means of the lattice-package in R (Sarkar, 2008). Pair correlation functions were obtained in simulation years where both functional types had similar densities to avoid potential side-effects. When carrying out interpretation it is important to recall that shifted and original positions are identical for PFT_rigid. We made allowance for graphical testing of statistical differences between the observed function and complete spatial randomness (CSR) using a confidence envelope built from 99 Monte Carlo simulations of a spatial Poisson process.

3. Results

3.1. Sensitivity analysis

The SA performed had two objectives. The first part is shown in the top half of Table 1 and it repeats an SA with the KiWi parameters to verify that the new model's behavior resembles that of the original one. In contrast, the SA shown in the bottom half of Table 1 involves newly introduced parameters. We intend to gain an understanding of the new routines for offspring production and disturbance frequency/intensity in accordance with the common objectives of SA, while the remainder of the article is devoted to the analysis of the plastic mangrove crown behavior.

The means for the stand state variables differ between SA-parts. The first part had means of tree density, stem volume (V), stand basal area (SBA), squared dbh (d_q), and dbh of the 100 thickest trees (dbh100) that were all higher than those in the second part. These differences were a consequence of the hurricane impacts that were present only in the second SA-part.

Among the growth parameters (b_2, b_3, g, dh_{max}) b_2 exerted the strongest effects on the stand state variables followed by dh_{max} and b_3. It is noteworthy, to report that reducing b_2 by 10% and raising b_3 by 10% caused runtime errors. Therefore, these two parameters were varied by only 5% in the problematic direction and the response to 10% variation was linearly extrapolated afterwards. However, in light of this issue we examined the meaning of these two parameters more closely. Essentially, the Shugart growth function is controlled by three easy-to-measure parameters: The initial maximum growth rate G, the maximum attained diameter at breast height (d_{max}) and height (h_{max}). In contrast, b_2 and b_3 represent only auxiliary variables, which are defined in terms of d_{max} and h_{max}. Hence, they should not be varied. Respective results are provided here only for comparison with previous SA, but are ignored in further interpretation.

The sole growth parameter of relevance, though, is dh_{max} (i.e. $d_{max} \times h_{max}$). Its variation affected the stem volume most strongly (−8.5%, +9.0%) and the stand basal area somewhat less strongly (−5.2%, +5.4%). These effects were mediated by corresponding differences of the squared diameter. Effects on the single state variable of the 100 thickest trees were lower, but in the same direction.

Table 2
Results of the linear mixed-effect models fitted on stand state variables of the monocultures (SD includes temporal variation within runs).

Treatment	Variable	PFT_rigid			PFT_plastic			Change	
		Mean	SD	SE	Mean	SD	SE	*p*-value, sign	± %
Without_Disturbance	stem volume [m^3 ha^{-1}]	621.86	14.22	0.30	663.42	14.34	0.22	0.0001***	6.68
	Density [ha^{-1}]	843.89	12.71	0.21	847.45	14.18	0.15	0.0033**	0.42
	Competition ($\times 10^6$)	193.29	7.18	0.18	189.59	7.67	0.13	0.0023**	−1.92
With_Disturbance	stem volume [m^3 ha^{-1}]	333.01	17.29	0.69	374.72	18.44	0.49	0.0003***	12.52
	density [ha^{-1}]	746.24	26.16	0.83	801.87	27.85	0.59	0.0002***	7.45
	competition ($\times 10^6$)	122.90	8.19	0.40	98.16	6.18	0.28	0.0003***	−20.14

Treatment	PFT_rigid positions	Original			Shifted			Change	
		Mean	SD	SE	Mean	SD	SE	*p*-value, sign	± %
Without_Disturbance	Clark–Evans index	1.268	0.012	0.003	1.302	0.010	0.004	0.0141*	2.73
	Canopy coverage [%]	78.50	0.42	–	79.85	0.45	–	–	1.72
	Canopy area [%]	84.51	1.12	–	84.51	1.12	–	–	0.00
With_Disturbance	Clark–Evans index	1.205	0.011	0.003	1.259	0.013	0.004	0.0051**	4.46
	Canopy coverage [%]	57.81	1.93	–	59.66	2.02	–	–	3.20
	Canopy area [%]	57.54	1.47	–	57.54	1.47	–	–	0.00

* $p < .05$.
** $p < .01$.
*** $p < .001$.

Varying the no. of seeds parameter had moderate effects only on the stand density (±5.6%).

Among the FON parameters I_{max} and I_{min} had almost negligible influence. The model, however, was most sensitive to the allometric exponent *b* and the allometric coefficient *a*, which scale the FON size to the *rbh* of the trunk. The sensitivity reached up to 25.4%. Effects were strongest on density, but somewhat less on SBA and *V*. The parameters control primarily the state variable of large trees (dbh100). In contrast to constant a, reduction of *b* led to an increase of stand state variables. This was due to the fact that both, the exponent *b* and *rbh*, are less than 1.

Among the newly introduced parameters (bottom half of Table 1) disturbance intensity as well as disturbance frequency exerted a considerable influence on the stand in the order density > *V* > SBA > dbh100 > d_q. However, due to the presence of non-linearity mesoFON was most sensitive to the new parameter propagule/sapling density per crown surface area. The respective sensitivity ranged from −15.8 to +14.4%.

In summary, according to the SA every effort shall be made in the near future to get more control over the FON-sizing parameters (*a*, *b*) and the seed density parameter, respectively.

3.2. Monoculture experiments

These simulation experiments were conducted to determine whether red mangrove crown plasticity enhances the carrying capacity or reduces the competitive strength of the system and whether disturbance alters this dichotomy. The top half of Table 2 shows results of the linear mixed-effects models fitted to stand state variables of the monocultures. Because of the low variation among the two repetitive runs (after temporal pseudo-replication was accounted for) all differences between the plastic and the rigid functional type were highly significant.

Crown plasticity enhanced the stand-based stem volume substantially by 6.68% in the dense red mangrove stands that form Without_Disturbance, whereas tree density was only marginally affected and the average competition strength in the stand decreased only slightly. Therefore, under these conditions crown displacement primarily raised the carrying capacity in terms of the stem volume. This was due to a surge in the average tree size of the red mangroves.

Impacted red mangrove stands, by contrast, developed a 45% lower stand-based stem volume than non-impacted stands, however, only 12% fewer trees were present in the stands, indicating a strong regenerative response to the hurricane impacts. Basically, the stand state response to crown plasticity in stands with disturbance was quite different than for stands without disturbance. Crown movement greatly reduced the competitive strength (−20.14%) and sharply raised tree density. Therefore, crown displacement improved the closure of gaps formed by the disturbance. The carrying capacity was stimulated, in terms of both stem volume (+12.52%) and tree density (+7.45%).

The bottom half of Table 2 shows results of the point pattern and canopy coverage analysis. In both analyses patterns of shifted positions are compared with those at original positions. The point pattern of the shifted positions had a higher Clark–Evans aggregation index than the original positions, irrespective of the disturbance regime, meaning that the "shifted" pattern was more regularly distributed in space than the original pattern. However, the indices for without disturbance tended to be larger than those for with disturbance, due to the higher tree density in the Without_Disturbance treatment.

Canopy coverage shows a trend that is similar to the aggregation index. The ground area covered by crowns located at their centroids is larger than expected. as if they were located at their stem bases. Therefore, the projections of shifted crowns tended to overlap less and make better use of the available space than did the original ones. Canopy coverage was noticeably lower than the summed crown area in the undisturbed treatment. Therefore, crown projections located at shifted or original positions showed considerable overlap in this treatment. This was not the case in the disturbance treatment, where the canopy area was slightly smaller than the canopy coverage (by chance).

The higher canopy coverage of the shifted crowns is surprising when we recall that the red mangrove stand under study was an old-growth forest from which mature trees were eradicated by natural death from time to time. Crowns of smaller trees in the surrounding area had moved away from such a mature tree due to size-asymmetric competition; then, after the death of the mature tree the smaller trees redirected themselves and slowly closed the gap. Fig. 3 illustrates such behavior. Certainly, original crowns tend to have higher coverage at the margins of those gaps.

Fig. 4 shows the displacement distances realized by the red mangrove crowns as a box-and-whisker-plot. The most striking result is that small trees below a dbh of 40.2 cm tended to have higher absolute displacement distances without disturbance than with disturbance (Fig. 4a). Trees showed this behavior despite the fact that the effects of crown plasticity on stand state variables were

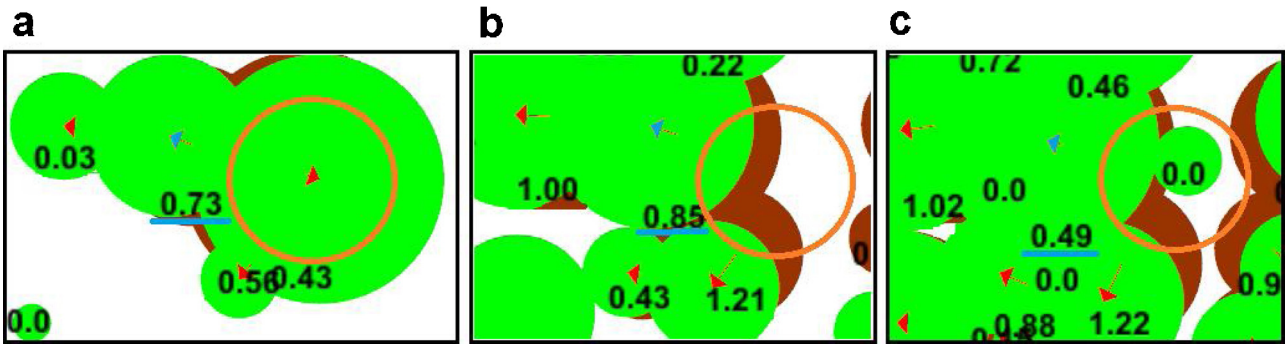

Fig. 3. Crown displacement close to a gap that formed by natural tree death: (a) 10 years before natural death a neighboring tree has shifted away from the mature tree (with circle) by 0.73 m (see underlined label). (b) In the year the mature tree dies the neighboring tree has displaced away from the gap by 0.85 m. (c) 20 years later the neighbor tree has redirected itself toward the gap, its displacement amounts to not more than 0.49 m.

more pronounced in monocultures with disturbance (see above). The same trend is evident in the relative displacement distances (Fig. 4b). Overall, displacement distances rose with tree size up to a dbh of 29.5 cm. The medians reached their maximum values at this size. They amounted to 0.84 m and 0.75 m (relative: 0.5 and 0.38) in the Without_Disturbance and With_Disturbance treatment. Absolute distances tended to level off for larger trees, whereas relative distances declined again in that range, because crown radii kept growing there.

In summary, the monoculture experiments demonstrate that even moderate crown plasticity is able to ameliorate competition and boost the carrying capacity in disturbed red mangrove stands due to its gap filling effect. In contrast, effects of massive crown plasticity on competition and less so on carrying capacity are confined in dense old-growth stands of that species.

3.3. Community experiments

We tested whether the advantage that PFT_plastic has shown in monoculture leads to a dominance of that functional type when grown in a community with PFT_rigid with these simulation runs. The fractions of initial saplings were varied widely for the two functional types involved in these runs.

Fig. 5 shows the time curses of the stand-based stem volume that developed with increasing numbers of PFT_rigid saplings from the top to the bottom row. The trajectories that arose without disturbance are illustrated on the left hand side, whereas those developing with disturbance are depicted on the right hand side. Apparently, the functional type with the capability to move the crown was able to competitively exclude the rigid type over the long term in all these runs. Generally, the lower the initial number of PFT_plastic saplings the longer competitive exclusion took. However, the time to PFT_rigid extinction was also severely influenced by the disturbance regime. The time to extinction ranged from $1840 \pm SD = 115$ to 3940 ± 764 years in the Without_Disturbance and from 2448 ± 1188 to 9677 ± 445 years in the With_Disturbance regime. Hurricane impacts accelerated the time to extinction by a factor of 2.39 on average with a standard deviation of ± 0.66. Competitive exclusion was absent and the community remained almost in balance in a model version in which the total annual propagule production was recorded and allocated in equal shares to both functional types (data not shown here). Therefore, we can state that the superiority of PFT_plastic stands was primarily due to a better fitness of plastic red mangrove individuals.

We sought to gain an understanding of how patterns interact with processes and how the interaction shapes the communities by using the pair correlation function (pcf) on the point patterns of shifted crown positions. Fig. 6 shows the functions for the Without_Disturbance treatment in the top-right triangle of plots and those of the With_Disturbance treatment in the bottom-left triangle.

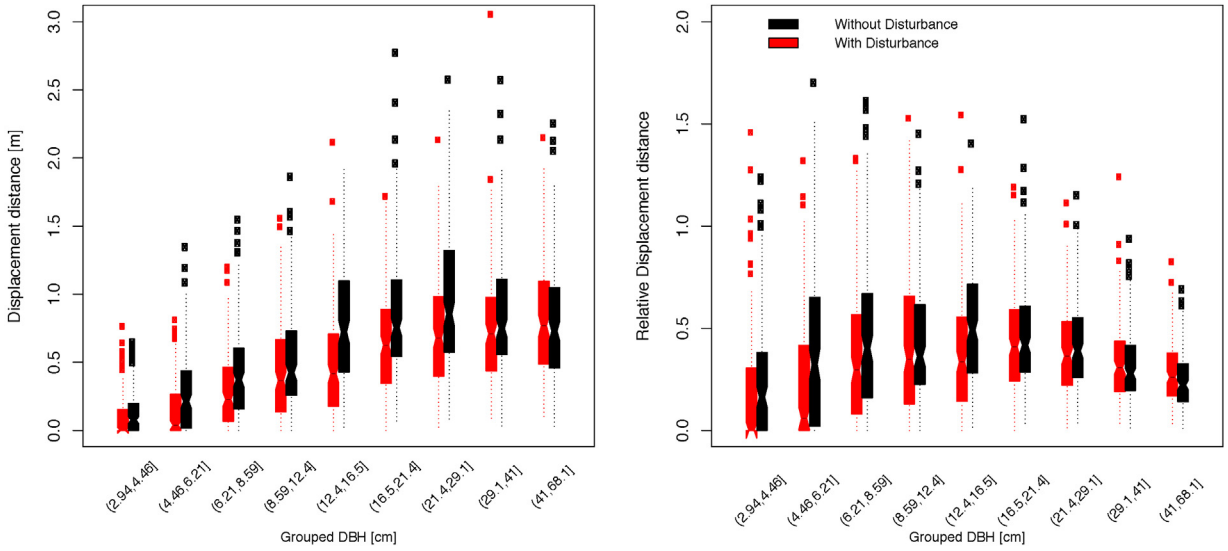

Fig. 4. Box and whisker plots of absolute (a) and relative (b) displacement distances for various tree groups classified according to their dbh in the Without_Disturbance and With_Disturbance treatment.

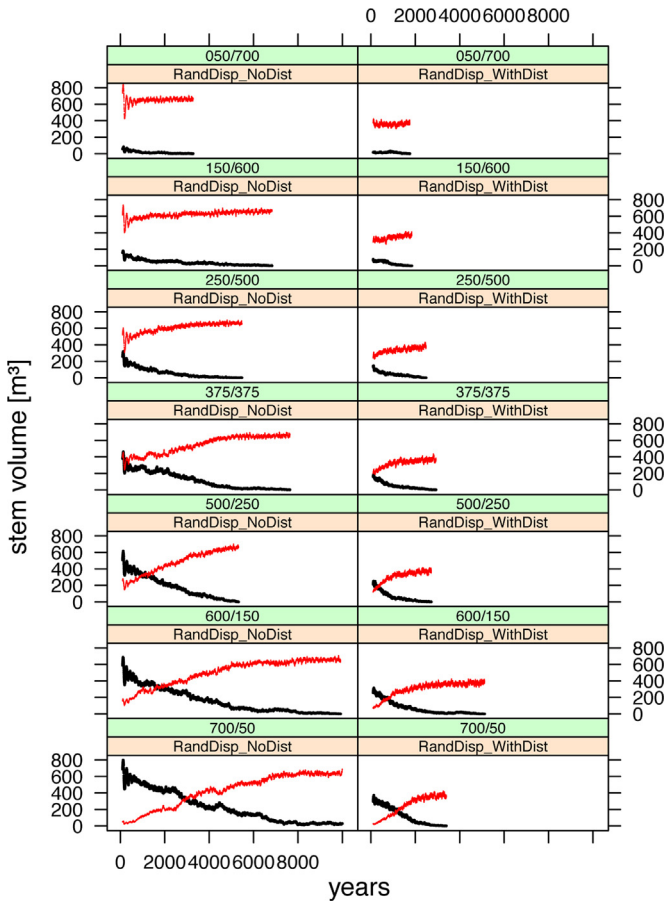

Fig. 5. Time course of the stand-based stem volume for PFT_plaastic (red) and PFT_rigid (black) when grown as a community: Without_Disturbance treatment is shown on the left hand side, With_Disturbance on the right. From the top to the bottom row the number of the PFT_rigid saplings planted initially increases. (For interpretation of reference to color in this figure legend, the reader is referred to the web version of this article.)

The pcf of PFT_rigid pairs was below the confidence envelope of complete spatial randomness (CSR, gray region) and did not enter the envelope until a distance of 3 m was reached in the Without_Disturbance treatment. Therefore, due to local competition, PFT_rigid was distributed regularly at low distances. However, at a distance of 4.5 m, the distribution became an aggregated one (pcf above the envelope). The pcf was inside the envelope at all other distances (up to 25 m) and belonged to the CSR distribution, as we might expect for an old-growth forest.

Obviously, the overall pcf trajectory remained very similar in PFT_plastic-PFT_plastic interactions. However, some differences did occur. Counter-intuitively, the regular region at low distances was narrow (envelope entry distance = 2 m) and the aggregated peak was more widespread and remained inside the envelope.

In PFT_plastic–PFT_rigid interactions the distribution at low distances was regular and – as above – the regular region was narrow. The aggregated peak was significant, although more widespread when compared with PFT_rigid interactions.

PFT_plastic also had a regular distribution at small distances (below 1.8 m) in the With_Disturbance treatment, irrespective of the interaction it was involved in. However, a down-shift of the envelope entry point was absent in this case. The aggregated peak is still visible in the pair correlation function of PFT_rigid, although it does not leave the envelope again in this treatment. In contrast, the peak was entirely absent anywhere PFT_plastic was involved.

In summary, patterns were more persistently altered by crown plasticity in the With_Disturbance regime than in the Without_Disturbance regime, whereas crowding exerted severe constraints on the patterns in dense stands. The plastic processes induced more regular patterns than the rigid one at low distance and the spreading of the aggregated peak. Admittedly, some of the patterns, such as the narrowing of the regular region in PFT_plastic interactions, were contrary to our expectations. Moreover, the occurrence of the aggregation peak requires further consideration (see Section 4).

4. Discussion

In this study, we introduced mesoFON, a novel individual-based mangrove forest dynamics model that incorporates mangrove crown plasticity using a simple approach that exclusively takes advantage of the fields-of-neighborhood (FON) approach for the first time.

We further extended the model with a separation of competition into above-/below-ground parts and an individual-based offspring production. We will begin this section with a discussion of results derived from the sensitivity analysis. This will be combined with an extensive evaluation of the newly implemented routines. The remainder of the discussion is focused on the first application of the model.

4.1. Sensitivity analysis

The first part of the SA revealed that the model is most sensitive to the FON-sizing parameters b and a. To a lesser extent it is sensitive to the growth parameters b_2 and dh_{max}.

In principle, there exist two KiWi sensitivity analyses for comparison (Kautz et al., 2011; Vogt, 2012). However, Vogt's (2012) results are rather difficult to compare to ours because she investigated a distinct species (*Avicennia germinans*) in her SA, varied input parameters far more (±50%,) and restricted her analysis to the initial 100 simulation years. Nevertheless, the input parameters that influenced tree density the most were the FON parameters a and I_{min}. Therefore, at least agreement is reached with respect to the parameter a. The influence of the maximum sapling growth parameter G and (eventually) I_{min} is presumably due to the limited time period considered in Vogt's SA.

The Kautz et al. (2011) SA, however, is more suitable for comparison to ours because the authors investigated the model response with the a species belonging to the same genus (*Rhizophora apiculata*) and varied parameters by the same amount ±10% than we did. Yet their SA differs from our SA in terms of the applied methodology (extended Fourier Amplitude Sensitivity Test vs. OAT-SA) and the restriction of the simulation period (initial 100 years as in Vogt, 2012). Kautz et al. found tree density to be most strongly affected by FON parameters a and b. The growth parameter b_3 was less influential (First Order effects only). Overall, results concerning a and b are in good quanitative agreement with ours. Results of growth parameters are in contrast to ours, but shall not be dealt with further here because b_2 and b_3 are only auxiliary variables that should not be varied (compare results). Essentially, we infer from the results that mesoFON behavior resembles KiWi behavior and take that as verification of successful implementation.

Based on the results of the first SA part, we will make every effort to gain more control over the FON-sizing parameters, because they are merely assumed and fine-tuned to the empirical data (Berger and Hildenbrandt, 2000). Fortunately, we have already moved quite far into this direction with the proposed separation into above-/below-ground FONs. In the future below-ground FON dimensions can be derived from dimensions of the rooting system because their

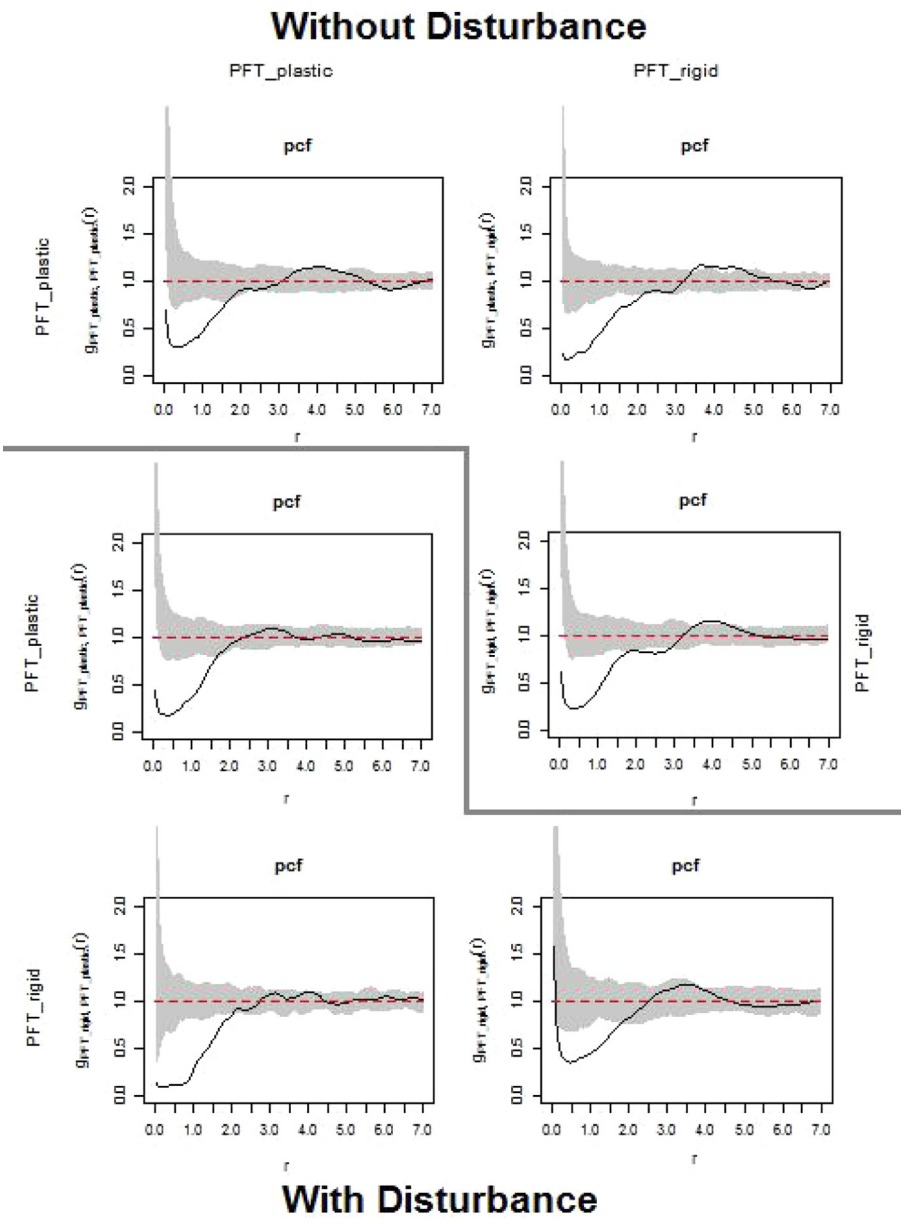

Fig. 6. Pair correlation functions for PFT_plastic:PFT_plastic, PFT_plastic:PFT_rigid and PFT_rigid:PFT_rigid neighbors in communities without disturbance (top-right triangle) and with disturbance (bottom-left triangle).

sizes match. We will even be able to measure the FON-sizing parameters above-ground for true mangroves due to their aerial roots and nearby clusters of fine roots (Tomlinson, 1994).

Arguments similar to those stated for the below-ground FON dimensions also hold for the above-ground FON dimensions. Imagine that competition for light is simulated in mesoFON as a shadow-fight on the forest ground with above-ground FONs representing the shadows of the crowns. The tight linkage between the dimensions of crown and above-ground FON that is necessary for this can be achieved by assuming that both have equal allometric exponents and proportional allomcetric constants (assumption of isometry). The better availability of crown allometric relationships will likely simplify above-ground FON parametrization.

We postpone the discussion of the strong model sensitivity to the newly introduced propagule density per crown surface area, which was the prime result of the second SA part, until the related evaluation section.

4.2. Evaluation of the separation into above-/below-ground FONs

A prerequisite for the implementation of crown plasticity was a separation into above- and below-ground competition.

Our intention was to keep the new parameterization consistent with the KiWi model FON-parameters that describe the integrated effects of both above- and below-ground competition, because they have been applied successfully to a number of case studies (Berger and Hildenbrandt, 2000; Berger et al., 2006; Piou et al., 2008, Kautz et al., 2011; Vogt, 2012).

In accordance with other individual-based forest growth models (SORTIE; Deutschman et al., 1997) we gave above-ground competition a far greater weighting than that operating below-ground (weighting ratio 3:1). We further assumed that competition for sunlight is highly asymmetrical (Grams and Andersen, 2007) and therefore assigned the above-ground I_{max} parameter to 0.95 and I_{min} to 0.07, i.e. the intensity of a competitive field drops sharply

from 0.95 at the trunk to 0.067 (in absolute terms) at the FON radius.

Below-ground competition for resources, in contrast to above-ground competition, is considered to be size-symmetrical (Casper and Jackson, 1997), when the nutrient under investigation is rather mobile and has a non-patchy distribution in the soil volume (Grams and Andersen, 2007). Therefore, to infer the symmetry of competition, one has to assess the mobility of the limiting ion in the rhizosphere of a *R. mangle* stand. Reef et al. (2010) reported nitrogen to be the factor limiting mangrove growth in half of the studies they cited, while in the other half phosphorous limitation was detected. However, there is one mesocosm study in which Fe^{2+} limited mangrove growth (Alongi, 2010).

The top 20 cm of the red mangrove rhizosphere have a redox potential of 100–200 mV (Marchand et al., 2004), which falls into the category "suboxic" or "moderately reducing." These conditions are characterized by high rates of N-fixation, ammonification, and denitrification (Reef et al., 2010). Therefore, the major nitrogen form prevailing under these conditions is ammonium. Saltwater cations occupy part of the soil binding sites, which makes the mobility of ammonium in mangrove soil substantially higher than that in terrestrial soil types. Furthermore, the product of prevalent Fe-reduction (Fe^{2+}) and phosphorous are released into the soil pore water under these conditions and are made available for plant uptake (Reef et al., 2010).

Therefore, we assume a sound mobility of all the limiting factors in the rhizosphere and infer a rather symmetrical type of below-ground competition at an overall low intensity. In line with that, I_{max} was assigned to 0.05 and I_{min} to 0.999 (0.05 in absolute terms). Both kinds of competition work additively in the program, therefore, we used combined FON parameters that closely resemble those used in the original model.

4.3. Evaluation of the propagule production

The second part of the SA, however, revealed that the propagule density per crown surface area exerted strong leverage on the model outcome. A default parameter setting was chosen to reflect the stand-based stem volume obtained with random recruitment. We simplified the propagule density to be constant over the lifetime of a tree in the optimum growth case, whereas a proportional decline was supposed when tree growth was constrained. We strongly believe that this latter regulation is mandatory to prevent the biologically unrealistic behavior that a tree at sub-optimal growing condition produces more propagules over its lifetime than in the optimal situation (compare Appendix C in Supplementary Material). Nevertheless, it is clear that this treatment requires the researchers to make serious assumptions about the ontogenetic variation of reproductive allocation. Variation related to environmental conditions as well as mast-year-like inter-annual variations have been reported for propagule production of *R. mangle* stands (Mehlig, 2006), but information about the ontogenetic variation of recruitment is currently lacking for this species. These are the reasons we applied the simple deterministic treatment of recruitment in this study.

However, because the crown radius in mesoFON is given by $r_{crown} = 0.636 \cdot 7.113 dbh^{0.654}$ and the surface area of a spherical crown is quadratically dependent on r_{crown} the reproductive allocation (N) scales with dbh as $N \sim dbh^{1.31}$. The resulting exponent of 1.31 tends to be rather low when compared with general trends and theoretical predictions. Analyses of the allometric relationships between reproductive allocation and stem diameter in trees revealed a range of allometric exponents from 1.7 to 2.2 (Thomas, 2011, gymnosperm and angiosperm species in Niklas, 1994). An exponent of 2 is also widely used in forest models (Pacala et al., 1993). Under the assumption that tree biomass (M) scales with stem diameter (D) as $M \sim D^{8/3}$ (Thomas, 2011), an exponent of 2 for reproductive mass lies below isometry, meaning, that reproduction declines with size. This contradicts general predictions of life-history theory that reproduction should increase with age and size in repeatedly reproducing organisms (Thomas, 2011), such as trees. However, the exponents vary to a large extent and even values of 5.3 have been reported for a number of species (Thomas, 2011). Unfortunately, we are currently lacking data on the propagule production of individual red mangrove trees over their entire lifetime. We may raise the propagule density with tree size such that reproductive allocation scales with dbh to the power of two, regardless of whether such information becomes available or not.

4.4. Evaluation of crown plasticity

We have taken a simple, two-dimensional modeling approach whose species-specific parameters can be easily determined from field measurements of crown projections because their competitive intensity declines exponentially with distance from a focal tree. Above-ground fields of neighborhood are ideally suited for simulating neighborhood asymmetry and related crown movement. We had to link movement, size of crown, and above-ground FON to establish a tight cause-effect relationship to make this function properly. Along with the separation of competition this ensures that locations and directions of interference are correctly reflected by the model. Our approach takes into account the species-specific size-asymmetry of above-ground competition that is an important determinant of variation in plasticity during ontogeny (Umeki, 1995a, 1997). It also does not require additional concepts as it reuses only those already available in the model.

The proposed methodology is similar to the crown-vector approach of Umeki (1995b), which is based on a vector addition of height-dependent zones of influence instead of FONs. Crown vectors are also used for the phototropism mechanism in the plastic versions of SORTIE (Strigul et al., 2008; Strigul, 2012). Umeki's model shares most of the advantages with mesoFON. However, it has some disadvantages relative to mesoFON in that it does not separate above-/below-ground competition it calculates displacement distances and directions with bias. Our model also has a close relationship to methods which calculate snapshots of neighborhood asymmetry and crown displacement from field data (Muth and Bazzaz, 2002), but our approach has the advantage of being dynamic.

Despite its simplicity our model surpasses others by accounting for both mechanisms responsible for crown displacement, specifically trunk bending and differential side branch growth (Muth and Bazzaz, 2002). mesoFON provides species-specific parameters for each of these.

Umeki (1997) was the first to consider the costs of crown plasticity by introducing a scalable penalty term that reduces the effective tree height and many have followed his lead. Umeki differentiates between a behavior in which a tree responds to the presence of a neighbor only after growth reduction has taken place (costly) and a behavior in which a tree's response precedes negative effects (not costly). Due to the advantages of the FON approach (competition declining with distance) we get this differentiation almost for free: Large sc_{bend} and sc_{crown} allow a tree to escape from negative effects and represent an almost cost-free response. Tree height, although functional in our model, was not suitable for implementation of costs as it had only minor effects. This is illustrated with the following rough estimation: We estimate the true height to be 33.13 m by applying Pythagoras' theorem for the maximum displacement distance case of about 3 m at a dbh of 35 cm (size class 29.5–40.2 cm) and a hypotenuse of 33.26 m (from Eq. (3)). However, much more movement is going on in the stand

than suggested by the displacement distances. We measured that one sixth of the trees touch the upper crown plasticity limit with the given plasticity parameters in each year.

Other more complex models incorporating crown plasticity have higher data requirements that are difficult to meet: WHORL, for example, requires information about module and branch growth (Sorrensen-Cothern et al., 1993; Umeki, 1995a); for the Plastic SORTIE and LES model information regarding the tessellation cell is needed (Strigul et al., 2008; Strigul, 2012). Recently, Vincent and Harja (2007) have even used sophisticated three-dimensional modeling to analyze the ecological significance of crown deformation on only one species (*Hevea brasiliensis*. Müll.Arg.). In contrast, the requirement specification for our approach required only simplicity, general applicability, and mechanistic basis.

4.5. Monoculture experiments

A number of field studies have investigated the influence of natural or anthropogenic disturbance on crown displacement (Young and Hubbell, 1991; Brisson, 2001; Longuetaud et al., 2008). Young and Hubbell in a study on crown plasticity of rainforest trees stated that "the crowns of most gap-edge trees were strongly asymmetric into their adjoining gaps" (Young and Hubbell, 1991, p. 1464). Brisson (2001) reported crown asymmetry of sugar maple (*Acer saccharum* Marsch.) to be highest along forest edges, intermediate around gaps and along new trails, and lowest for isolated trees. Longuetaud et al. (2008) found that the distribution of crown centers compared to the distribution of stem bases was most strongly shifted toward regularity at an intermediate thinning regime.

However, to the best of our knowledge, this is the first simulation study to target the interaction of disturbance and crown plasticity. In accordance with results of field studies we found larger effects of crown plasticity on the carrying capacity in disturbed monocultures. Crown shifts stimulated stand-based stem volume as well as tree density more in that treatment. The most striking result, however, was the drop in competition due to plasticity that occurred in disturbed stands. Obviously, trees with plastic responses were able to conquer gap space better than the rigid counterparts. The finding is in good agreement with the contribution of plastic response to gap closure found in field surveys (Young and Hubbell, 1991; Brisson, 2001, studies reviewed by Strigul, 2012). Inherently consistent and also in line with results of empirical studies (Longuetaud et al., 2008, 2013; Schröter et al., 2012) and modeling studies (Umeki, 1997; Strigul et al., 2008) are our findings (1) that distributions of crown centers are more regularly distributed than distributions of stem bases and (2) that crowns located at their center cover a larger ground area.

We believe one of the greatest advantages of individual-based models is that you can gain an understanding of the processes involved by visually following the development of the forest stand within minutes that in reality would take centuries. A good example is the observation that crowns of small red mangrove trees are pointed away from a gap immediately after it has formed by the natural death of a large mature tree and then slowly redirect themselves to close the gap. The behavior is plausible, but in the literature only the opposite, the "riverside behavior", i.e. the leaning toward a gap, has been described (Young and Hubbell, 1991; Strigul, 2012).

Given the overall larger effect size of crown displacement with disturbance it was astonishing at first that displacement distances were lower in that treatment. This can be explained by considering that displacement is less likely to occur in gaps. On the other hand, from the relative distances, we can assess whether setting the parameters sc_{bend} and sc_{crown} arbitrarily to 5 leads to realistic behavior. Longuetaud et al. (2008) found the average relative displacement for a variety of species to be 0.57 with a standard deviation of ±0.62. Longuetaud et al. found that common hornbeam (*Carpinus betulus*, L.) with a value of 0.61 ± 0.62 appeared to be a plastic species, whereas beech (*Fagus sylavatica*, L.) with 0.36 ± 0.76 seemed less responsive. Schröter et al. (2012) confirm the latter result by giving a mean of 0.37 for beech. With the given parameters we obtained here medians of 0.5 and 0.38 for *R. mangle* in the Without_Disturbance and With_Disturbance treatments. The values seem realistic as they fall well within the reported range. Field measurements of displacement distances to obtain real red mangrove parameters are underway.

4.6. Community experiments

Pair correlation functions have been recommended for the study of neighborhood density relationships in ecology (Stoyan and Stoyan, 1994; Wiegand and Moloney, 2013). We used the functions here to examine the processes underlying the observed pattern.

We found that patterns were more strongly and more persistently altered by crown plasticity in the With_Disturbance regime than in the Without_Disturbance regime, whereas crowding seemed to exert severe constraints on the patterns in the dense stands that formed without disturbance. The plastic processes induced more regular patterns at low distance (but not in all interactions) and the spreading of an aggregated peak at intermediate distance. However, an extension of the regular region to longer distances, a consequence of the plastic behavior observed in field studies (e.g. Schröter et al., 2012), was lacking here. We assume that this is due to the large variation of tree sizes in the old-growth forest under simulation. Complete spatial randomness is assumed to be the final stage of such a forest (Pommerening, 2002). That is why the occurrence of an aggregation peak was contrary to our expectations. The peak could be a consequence of the postulated circular FON-shape, but this would not explain the fact that it faded away in the PFT_plastic interaction with disturbance. Alternatively, we speculate that in dense stands a hotspot of sapling establishment is situated at this distance. Its disappearance with disturbance in PFT_plastic interactions then indicates better space usage for sapling establishment due to plasticity.

PFT_plastic was finally able to out-compete PFT_rigid in all experiments. The significance of the morphological plasticity for the coexistence of PFTs in the long run has been demonstrated here for the first time. The higher fitness of the plastic individuals was primarily mediated by an enhanced fecundity of the taller trees (unpublished data). Hurricane impacts, in particular, accelerated community dynamics strongly and diminished massively the time to PFT_rigid extinction. Mangrove forests are subject to frequent disturbance at all scales (Alongi, 2008). Mangrove species (of the neo-tropics) are known to possess contrasting growth strategies that are commonly associated with the magnitude of crown plasticity (McKee, 1995; Berger et al., 2006; Strigul, 2012). Our results indicate that crown plasticity may also play a role for species coexistence in those ecosystems. The question whether crown plasticity affects processes at the community level has recently been addressed for the first time. By combining rainforest biodiversity experiments with individual-based modeling Sapijanskas et al. (2014) demonstrated that temporal niche differences and crown plasticity were responsible for changes in ecosystem functioning. Inspired by this work, we contemplate to pass our promising results on to the next level, calibrate mesoFON for several neo-tropical mangrove species and explore crown plasticity effects at the mangrove community level.

Acknowledgements

We would like to thank the editor and two anonymous reviewers for their constructive suggestions that helped improving

the manuscript. The German Research Foundation (Deutsche Forschungsgemeinschaft) provided funding for this project (research grant: DFG BE 1960/7-1). The European Commission funded the international cooperation within this study through the "Coastal Research Network on Environmental Changes" (CREC) as part of its 7th Framework Program. The CREC project is classified as a Marie Curie Action (FP7-PEOPLE-2009-IRSES).

Appendix A. Supplementary data

Supplementary material related to this article can be found, in the online version, at http://dx.doi.org/10.1016/j.ecolmodel.2014.07.014.

References

Alongi, D.M., 2008. Mangrove forests: resilience, protection from tsunamis, and responses to global climate change. Estuar. Coast. Shelf Sci. 76, 1–13.
Alongi, D.M., 2010. Dissolved iron supply limits early growth of estuarine mangroves. Ecology 91, 3229–3241.
Baddeley, A., Turner, R., 2005. spatstat: An R package for analyzing spatial point patterns. J. Stat. Softw. 12, 1–42.
Berger, U., Hildenbrandt, H., 2000. A new approach to spatially explicit modelling of forest dynamics: spacing, ageing and neighbourhood competition of mangrove trees. Ecol. Modell. 132, 287–302.
Berger, U., Adams, M., Grimm, V., Hildenbrandt, H., 2006. Modelling secondary succession of neotropical mangroves: causes and consequences of growth reduction in pioneer species. Perspect. Plant Ecol. Evol. Syst. 7, 243–252.
Berger, U., Rivera-Monroy, V.H., Doyle, T.W., Dahdouh-Guebas, F., Duke, N.C., Fontalvo-Herazo, M.L., Hildenbrandt, H., Koedam, N., Mehlig, U., Piou, C., Twilley, R.R., 2008. Advances and limitations of individual-based models to analyze and predict dynamics of mangrove forests: a review. Aqua. Bot. 89, 260–274.
Borges, R., 2008. Plasticity comparisons between plants and animals. Concepts Mech.
Botkin, D.B., Janak, J.F., Wallis, J.R., 1972. Rationale, limitations, and assumptions of a northeastern forest growth simulator. IBM J. Res. Dev. 16, 101–116.
Bradshaw, A.D., 2006. Unravelling phenotypic plasticity? Why should we bother? N. Phytol. 170, 644–648.
Brisson, J., 2001. Neighborhood competition and crown asymmetry in Acer saccharum. Can. J. For. Res. 31, 2151–2159.
Casper, B.B., Jackson, R.B., 1997. Plant competition underground. Annu. Rev. Ecol. Syst. 28, 545–570.
Chen, R., Twilley, R.R., 1998. A gap dynamic model of mangrove forest development along gradients of soil salinity and nutrient resources. J. Ecol. 86, 37–51.
Clark, P.J., Evans, F.C., 1954. Distance to nearest neighbor as a measure of spatial relationships in populations. Ecology 35, 445.
Deutschman, D.H., Levin, S.A., Devine, C., Buttel, L.A., 1997. Scaling from trees to forests: analysis of a complex simulation model. In: Science Online, http://www.sciencemag.org/site/feature/data/deutschman/index.htm
Fontalvo-Herazo, M.L., Piou, C., Vogt, J., Saint-Paul, U., Berger, U., 2011. Simulating harvesting scenarios towards the sustainable use of mangrove forest plantations. Wetlands Ecol. Manage. 19, 397–407.
Grams, T.E.E., Andersen, C.P., 2007. Competition for resources in trees: physiological versus morphological plasticity. Progress in Botany, 68. Springer-Verlag, Berlin, pp. 356–381.
Grimm, V., Railsback, S.F., 2005. Individual-based Modeling and Ecology, vol. xvi. Princeton University Press, Princeton, pp. 428.
Grimm, V., Berger, U., Bastiansen, F., Eliassen, S., Ginot, V., Giske, J., Goss-Custard, J., Grand, T., Heinz, S.K., Huse, G., Huth, A., Jepsen, J.U., Jørgensen, C., Mooij, W.M., Müller, B., Pe'er, G., Piou, C., Railsback, S.F., Robbins, A.M., Robbins, M.M., Rossmanith, E., Rüger, N., Strand, E., Souissi, S., Stillman, R.A., Vabø, R., Visser, U., DeAngelis, D.L., 2006. A standard protocol for describing individual-based and agent-based models. Ecol. Modell. 198, 115–126.
Grimm, V., Berger, U., DeAngelis, D.L., Polhill, J.G., Giske, J., Railsback, S.F., 2010. The ODD protocol: a review and first update. Ecol. Modell. 221, 2760–2768.
Grote, R., Pretzsch, H., 2002. A model for individual tree development based on physiological processes. Plant Biol. 4, 167–180.
Kautz, M., Berger, U., Stoyan, D., Vogt, J., Khan, N.I., Diele, K., Saint-Paul, U., Triet, T., Nam, V.N., 2011. Desynchronizing effects of lightning strike disturbances on cyclic forest dynamics in mangrove plantations. Aqua. Bot. 95, 173–181.
Khan, M.N.I., Sharma, S., Berger, U., Koedam, N., Dahdouh-Guebas, F., Hagihara, A., 2013. How do tree competition and stand dynamics lead to spatial patterns in monospecific mangroves? Biogeosciences 10, 2803–2814.
Longuetaud, F., Seifert, T., Leban, J.-M., Pretzsch, H., 2008. Analysis of long-term dynamics of crowns of sessile oaks at the stand level by means of spatial statistics. For. Ecol. Manage. 255, 2007–2019.
Longuetaud, F., Piboule, A., Wernsdörfer, H., Collet, C., 2013. Crown plasticity reduces inter-tree competition in a mixed broadleaved forest. Eur. J. For. Res. 132, 621–634.
Marchand, C., Baltzer, F., Lallier-Vergès, E., Albéric, P., 2004. Pore-water chemistry in mangrove sediments: relationship with species composition and developmental stages (French Guiana). Mar. Geol. 208, 361–381.
McKee, K.L., 1995. Interspecific variation in growth, biomass partitioning, and defensive characteristics of neotropical mangrove seedlings: response to light and nutrient availability. Am. J. Bot. 82, 299.
Mehlig, U., 2006. Phenology of the red mangrove, *Rhizophora mangle* L., in the Caeté Estuary, Pará, equatorial Brazil. Aqua. Bot. 84, 158–164.
Muth, C.C., Bazzaz, F.A., 2002. Tree canopy displacement at forest gap edges. Can. J. For. Res. 32, 247–254.
Niklas, K.J., 1994. Plant Allometry. The Scaling of Form and Process, vol. xvi. University of Chicago Press, Chicago, pp. 395.
North, M.J., Collier, N.T., Ozik, J., Tatara Eric, R., Macal Charles, M., Bragen, M., Sydelko, P., 2013. Complex adaptive systems modeling with repast simphony. Complex Adap. Syst. Model. SpringerOpen J. http://www.casmodeling.com/content/1/1/3
Pacala, S.W., Canham, C.D., Silander Jr., J.A., 1993. Forest models defined by field measurements. I. The design of a northeastern forest simulator. Can. J. For. Res. 23, 1980–1988.
Pacala, S.W., Canham, C.D., Saponara, J., Silander, J.A.JJr., Kobe, R.K., Ribbens, E., 1996. Forest models defined by field measurements: Estimation, error analysis and dynamics. Ecol. Monogr. 66, 1.
Peck, A., 2008. Beginning GIMP: From Novice to Professional. Apress Media LLC, New York City.
Pinheiro, J., Bates, D., DebRoy, S., Sarkar, D., R Development Core Team, 2012. nlme: Linear and Nonlinear Mixed Effects Models. R package version 3.1-103, http://cran.r-project.org/web/packages/nlme/index.html
Piou, C., Berger, U., Hildenbrandt, H., Feller, I.C., 2008. Testing the intermediate disturbance hypothesis in species-poor systems: a simulation experiment for mangrove forests. J. Vegetat. Sci. 19, 417–424.
Pommerening, A., 2002. Approaches to quantifying forest structures. Forestry 75, 305–324.
Pretzsch, H., 2009. Forest Dynamics, Growth and Yield. From Measurement to Model, vol. XIX. Springer, Berlin/Heidelberg, pp. 664.
R Development Core Team, 2012. R: A Language and Environment for Statistical Computing, http://www.R-project.org.
Reef, R., Feller, I.C., Lovelock, C.E., 2010. Nutrition of mangroves. Tree Physiol. 30, 1148–1160.
Robert, E.M.R., Schmitz, N., Okello, J.A., Boeren, I., Beeckman, H., Koedam, N., 2011. Mangrove growth rings: fact or fiction? Trees 25, 49–58.
Saltelli, A., 1999. Sensitivity analysis: could better methods be used? J. Geophys. Res. 104, 3789.
Sapijanskas, J., Paquette, A., Potvin, C., Kunert, N., Loreau, M., 2014. Tropical tree diversity enhances light capture through crown plasticity and spatial and temporal niche differences. Ecology, in press.
Sarkar, D., 2008. Extending lattice: using generics and methods to implement new visualization methods within the Trellis framework. Comput. Stat. 23, 565–572.
Schröter, M., Härdtle, W., Oheimb, G., 2012. Crown plasticity and neighborhood interactions of european beech (*Fagus sylvatica* L.) in an old-growth forest. Eur. J. For. Res. 131, 787–798.
Shugart, H.H., 1984. A Theory of Forest Dynamics. The Ecological Implications of Forest Succession Models, vol. xiv. Springer-Verlag, New York, pp. 278.
Smith, T.J., Anderson, G.H., Balentine, K., Tiling, G., Ward, G.A., Whelan, K.R.T., 2009. Cumulative impacts of hurricanes on Florida mangrove ecosystems: sediment deposition, storm surges and vegetation. Wetlands 29, 24–34.
Sorrensen-Cothern, K.A., Ford, E.D., Sprugel, D.G., 1993. A model of competition incorporating plasticity through modular foliage and crown development. Ecol. Monogr. 63, 277.
Stoyan, D., Stoyan, H., 1994. Fractals, random shapes, and point fields. Methods of Geometrical Statistics, vol. xiv. Wiley, Chichester, New York, pp. 389.
Strigul, N., 2012. Individual-based models and scaling methods for ecological forestry: implications of tree phenotypic plasticity. In: García, J.M., Diez Casero, J.J. (Eds.), Sustainable Forest Management. Current Research. InTech, Rijeka.
Strigul, N., Pristinski, D., Purves, D., Dushoff, J., Pacala, S., 2008. Scaling from trees to forests: tractable macroscopic equations for forest dynamics. Ecol. Monogr. 78, 523–545.
Thomas, S.C., 2011. Age-Related Changes in Tree Growth and Functional Biology: The Role of Reproduction, Size- and Age-Related Changes in Tree Structure and Function, vol. 4. Springer, Dordrecht/New York, pp. 33–64.
Tomlinson, P.B., 1994. The Botany of Mangroves, vol. VIII. Cambridge University Press, Cambridge, pp. 419.
Trewavas, A., 2005. Plant intelligence. Naturwissenschaften 92, 401–413.
Umeki, K., 1995a. A comparison of crown asymmetry between *Picea abies* and *Betula maximowicziana*. Can. J. For. Res. 25, 1876–1880.
Umeki, K., 1995b. Importance of crown position and morphological plasticity in competitive interaction in a population of *Xanthium canadense*. Ann. Bot. 75, 259–265.
Umeki, K., 1997. Effect of crown asymmetry on size–structure dynamics of plant populations. Ann. Bot. 79, 631–641.
Valladares, F., Gianoli, E., Gómez, J.M., 2007. Ecological limits to plant phenotypic plasticity. N. Phytol. 176, 749–763.
Vincent, G., Harja, D., 2007. Exploring ecological significance of tree crown plasticity through three-dimensional modelling. Ann. Bot. 101, 1221–1231.
Vogt, J., Ph.D. thesis 2012. Modeling gap dynamics, succession, and disturbance regimes of mangrove forests. Fakultät Forst-, Geo- und Hydrowissenschaften, Technische Universität Dresden.
Wiegand, T., Moloney, K., 2013. Handbook of Spatial Point-Pattern Analysis in Ecology. Taylor & Francis.
Young, T.P., Hubbell, S.P., 1991. Crown asymmetry, treefalls, and repeat disturbance of broad-leaved forest gaps. Ecology 72, 1464.